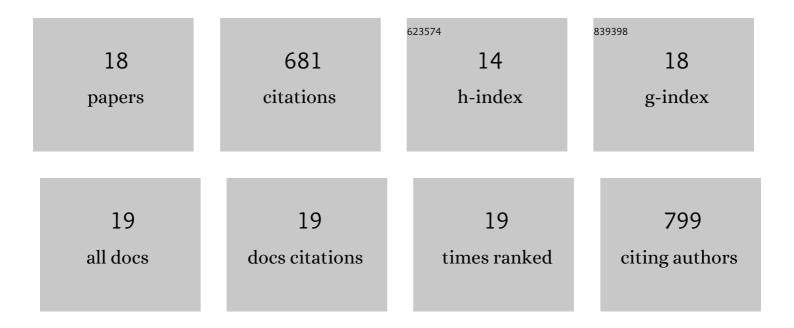
Sridharan Balu

List of Publications by Year in descending order

Source: https://exaly.com/author-pdf/2405674/publications.pdf Version: 2024-02-01



#	Article	IF	CITATIONS
1	Rational synthesis of BixFe1â^'xVO4 heterostructures impregnated sulfur-doped g-C3N4: A visible-light-driven type-II heterojunction photo(electro)catalyst for efficient photodegradation of roxarsone and photoelectrochemical OER reactions. Applied Catalysis B: Environmental, 2022, 304, 120852.	10.8	46
2	Photo–Redox Properties of –SO3H Functionalized Metal-Free g-C3N4 and Its Application in the Photooxidation of Sunset Yellow FCF and Photoreduction of Cr (VI). Catalysts, 2022, 12, 751.	1.6	6
3	Zinc and Sulfur Codoped Iron Oxide Nanocubes Anchored on Carbon Nanotubes for the Detection of Antitubercular Drug Isoniazid. ACS Applied Nano Materials, 2021, 4, 4562-4575.	2.4	25
4	Synthesis of novel and environmental sustainable AgI-Ag2S nanospheres impregnated g-C3N4 photocatalyst for efficient degradation of aqueous pollutants. Applied Surface Science, 2020, 500, 143991.	3.1	59
5	Tin disulfide nanorod-graphene-l²-cyclodextrin nanocomposites for sensing dopamine in rat brains and human blood serum. Materials Science and Engineering C, 2020, 108, 110367.	3.8	31
6	Sonochemical synthesis and anchoring of zinc oxide on hemin-mediated multiwalled carbon nanotubes-cellulose nanocomposite for ultra-sensitive biosensing of H2O2. Ultrasonics Sonochemistry, 2020, 63, 104917.	3.8	20
7	Morphology-Controlled Synthesis of α–Fe2O3 Nanocrystals Impregnated on g-C3N4–SO3H with Ultrafast Charge Separation for Photoreduction of Cr (VI) Under Visible Light. Environmental Pollution, 2020, 267, 115491.	3.7	39
8	Effect of ultrasound-induced hydroxylation and exfoliation on P90–TiO2/g-C3N4 hybrids with enhanced optoelectronic properties for visible-light photocatalysis and electrochemical sensing. Ceramics International, 2020, 46, 18002-18018.	2.3	31
9	Synthesis of sol–gel derived holmium aluminium garnet on exfoliated g-C3N4: a novel visible-light-driven Z-scheme photocatalyst for the degradation of sunset yellow FCF. Journal of Materials Science: Materials in Electronics, 2019, 30, 20132-20143.	1.1	6
10	Synthesis of boron doped C3N4/NiFe2O4 nanocomposite: An enhanced visible light photocatalyst for the degradation of methylene blue. Results in Physics, 2019, 12, 1238-1244.	2.0	46
11	Sonochemical synthesis of gum guar biopolymer stabilized copper oxide on exfoliated graphite: Application for enhanced electrochemical detection of H2O2 in milk and pharmaceutical samples. Ultrasonics Sonochemistry, 2019, 56, 254-263.	3.8	29
12	Synthesis of Flower-Like Iron Oxide Capped Tripolyphosphate for Electrochemical Detection of Carbadox Drugs in Meat. Journal of the Electrochemical Society, 2019, 166, B555-B561.	1.3	6
13	Synthesis of α-Fe2O3 decorated g-C3N4/ZnO ternary Z-scheme photocatalyst for degradation of tartrazine dye in aqueous media. Journal of the Taiwan Institute of Chemical Engineers, 2019, 99, 258-267.	2.7	95
14	Novel electrochemical synthesis of cellulose microfiber entrapped reduced graphene oxide: A sensitive electrochemical assay for detection of fenitrothion organophosphorus pesticide. Talanta, 2019, 192, 471-477.	2.9	55
15	Facile synthesis of cellulose microfibers supported palladium nanospindles on graphene oxide for selective detection of dopamine in pharmaceutical and biological samples. Materials Science and Engineering C, 2019, 98, 256-265.	3.8	28
16	Enhanced reversible redox activity of hemin on cellulose microfiber integrated reduced graphene oxide for H2O2 biosensor applications. Carbohydrate Polymers, 2019, 204, 152-160.	5.1	34
17	Assembly of ZnO Nanoparticles on SiO2@α-Fe2O3 Nanocomposites for an Efficient Photo-Fenton Reaction. Inorganics, 2018, 6, 90.	1.2	14
18	Degradation of Methylene Blue Dye in the Presence of Visible Light Using SiO2@α-Fe2O3 Nanocomposites Deposited on SnS2 Flowers. Materials, 2018, 11, 1030.	1.3	111